The American Journal of Pathology, Vol. 186, No. 3, March 2016

ELSEVIER

The American Journal of PATHOLOGY

ajp.amjpathol.org

METABOLIC, ENDOCRINE, AND GENITOURINARY PATHOBIOLOGY

Lack of p47^{phox} in Akita Diabetic Mice Is Associated with Interstitial Pneumonia, Fibrosis, and Oral Inflammation

Mai F. Zamakhchari,* Corneliu Sima,†‡ Kishore Sama,* Noah Fine,§ Michael Glogauer,§ Thomas E. Van Dyke,†‡ and Robert Gyurko*¶

From the Department of Periodontology and Oral Biology, Henry M. Goldman School of Dental Medicine, Boston University, Boston, Massachusetts; the Department of Applied Oral Sciences,† The Forsyth Institute, Cambridge, Massachusetts; the Department of Oral Medicine, Infection, and Immunity,‡ Harvard School of Dental Medicine, Boston, Massachusetts; The Matrix Dynamics Group,§ University of Toronto, Toronto, Ontario, Canada; and the Department of Periodontology,¶ Tufts University School of Dental Medicine, Boston, Massachusetts*

Accepted for publication October 29, 2015.

Address correspondence to Robert Gyurko, D.M.D., Ph.D., Tufts University School of Dental Medicine, 1 Kneeland St, Boston, MA 02111. E-mail: robert.gyurko@tufts.edu.

Excess reactive oxygen species production is central to the development of diabetic complications. The contribution of leukocyte reactive oxygen species produced by the NADPH oxidase to altered inflammatory responses associated with uncontrolled hyperglycemia is poorly understood. To get insight into the role of phagocytic superoxide in the onset of diabetic complications, we used a model of periodontitis in mice with chronic hyperglycemia and lack of leukocyte p47^{phox} (Akita/Ncf1) bred from C57BL/6-*Ins2*^{Akita}/J (Akita) and neutrophil cytosolic factor 1 knockout (Ncf1) mice. Akita/Nfc1 mice showed progressive cachexia starting at early age and increased mortality by six months. Their lungs developed infiltrative interstitial lesions that obliterated air spaces as early as 12 weeks when fungal colonization of lungs also was observed. Neutrophils of Akita/Ncf1 mice had normal degranulation and phagocytic efficiency when compared with wild-type mice. Although Akita/Ncf1 mice had increased prevalence of oral infections and more severe periodontitis compared with wild-type mice, bone loss was only marginally higher compared with Akita and Ncf1 null mice. Altogether these results indicate that lack of leukocyte superoxide production in mice with chronic hyperglycemia results in interstitial pneumonia and increased susceptibility to infections. *(Am J Pathol 2016, 186: 659–670; http://dx.doi.org/10.1016/j.ajpath.2015.10.026)*

Diabetes mellitus (DM) is a chronic disease characterized by altered metabolic and endocrine pathways involved in the control of blood glucose levels resulting in hyperglycemia. DM affects nearly 10% of the US population, and another 25% have pre-DM characterized by sustained high blood glucose levels.[1] Uncontrolled hyperglycemia is regarded as the central player in the development of diabetic complications including nephropathy, neuropathy, retinopathy, cardiovascular diseases, peripheral vascular diseases, and periodontal diseases. Periodontal diseases are chronic polymicrobial inflammatory diseases characterized by a deregulated local inflammatory reaction to pathogenic subgingival biofilms and progressive destruction of periodontal supporting tissues resulting in edentulism. It is estimated that patients with poorly controlled DM are three times more likely to develop chronic periodontal diseases compared with normoglycemic individuals despite similar composition in subgingival biofilms.[2–4] Existing evidence suggests that hyperglycemia and dyslipidemia affect the innate immune system and favor a systemic low-grade inflammatory state that predisposes to the impaired clearance of pathogens.[5–7] The observation of high levels of advanced glycation end-products in gingiva of diabetic mice has led to the hypothesis that advanced glycation end-product–mediated activation of inflammatory pathways in periodontal tissues may explain in

Supported by USPHS grants DE016933 (R.G.) and DE015566 (T.E.V.D.) from the National Institute of Dental and Craniofacial Research, NIH.

M.F.Z. and C.S. contributed equally to this work.

Disclosures: None declared.

http://dx.doi.org/10.1016/j.ajpath.2015.10.026

part the role of chronic hyperglycemia in periodontal diseases.[8,9] However, the relative contribution of hyperglycemia and dyslipidemia in the onset of diabetic complication is not completely understood.

The Akita mouse is a monogenic mouse model of DM that mostly resembles human T1DM in pathogenesis and phenotype. The Akita mouse is a heterozygous carrier of a missense point mutation in *INS2* gene (Akita$^{WT/C96Y}$) with early onset hyperglycemia and progressive development of diabetic complications. Reduction in β-cell mass as a result of apoptotic death induced by Akita mutation occurs within the first month of life. Heterozygous Akita show the first signs of DM at 4 to 6 weeks when blood glucose levels increase progressively and polyuria is apparent. Males have an earlier onset and more severe hyperglycemia compared with females. By 12 weeks, blood glucose levels exceed 500 mg/dL, and by 10 months, Akita develop severe forms of diabetic complications.[10] The Akita mouse model of diabetes offers the advantage of investigating the mechanisms through which uncontrolled hyperglycemia contributes to the onset and progression of diabetic complications. This allows us to dissect the otherwise difficult to assess independent metabolic changes associated with DM, such as dyslipidemia.

Overproduction of reactive oxygen species (ROS) by the mitochondrial electron transport chain was proposed as a unifying mechanism for diabetic microvascular complications because it relates to all metabolic changes that occur in DM.[11–13] ROS are generated in multiple cellular components including mitochondria (consuming 90% of cellular oxygen), peroxisomes, and endoplasmic reticulum as by-products of the oxidative phosphorylation process. An estimated 0.2% to 2% of oxygen consumption during oxidative phosphorylation processes contribute to superoxide generation.[14,15] It is believed that ROS generation in mitochondria is tightly regulated under physiological conditions, and that it does not contribute significantly to cellular oxidative stress.[15,16] In diabetes, however, high intracellular levels of glucose generate high mitochondrial membrane potential and subsequent overproduction of superoxide. The latter inhibits glyceraldehyde 3-phosphate dehydrogenase, resulting in the accumulation of upstream intermediates in glycolysis that will be processed through pathways of glucose overutilization such as polyol, hexozamine, *de novo* synthesis of diacylglycerol, a cofactor of protein kinase C, and the formation of advanced glycation end-products from accumulating trioses. Nonetheless, ROS increase the local production of transforming growth factor beta 1, fibronectin, and plasminogen activator inhibitor 1 in renal cells, demonstrating a critical role in excessive extracellular deposition.[17–20]

Unlike the generation of ROS as by-product of physiological processes, the NADPH oxidase enzyme complex functions primarily as a superoxide-generating system in phagocytes (neutrophils and macrophages) in response to pathogen-mediated stimulation. Its critical role in innate host defense is demonstrated by the phenotypes of chronic granulomatous disease (CGD), a group of genetic disorders caused by mutations in one of the enzyme's subunits. NADPH oxidase function in CGD neutrophils is inhibited, resulting in lack of superoxide production. CGD patients experience recurrent severe infections that may lead to life-threatening sepsis.[21] Upon neutrophil activation by pathogen-derived factors and phagocytosis, the cytoplasmic subunit p47^{phox} (also known as Ncf1) is phosphorylated at multiple serine residues, which leads to its assembly with other cytosolic subunits (p67^{phox} and p40^{phox}) and transfer to the cell membrane–bound cytochrome b558 to form active NADPH oxidase. Superoxide produced by NADPH oxidase is highly reactive and quickly catalyzes the formation of other ROS, such as hydrogen peroxide, hypochlorous acid, or peroxynitrite. In the absence of stimuli, virtually all p47^{phox} remains in the cytoplasm, precluding any superoxide production. In diabetic Akita mice, however, NADPH oxidase is preactivated by hyperglycemia because the p47^{phox} subunit is partially translocated to the cell membrane of unstimulated neutrophils, which results in a significantly higher release of superoxide in the absence of stimulation.[22] Similar premature assembly and priming of the NADPH oxidase was demonstrated in human neutrophils.[23,24] These findings indicated that hyperglycemia may mediate oxidative stress and the onset of diabetic complications by stimulating the ectopic release of neutrophil superoxide, particularly at sites with high levels of physiological neutrophil trafficking, such as biofilm-bearing tissues.

The relative contribution of NADPH-derived and mitochondrial excess ROS to the pathogenesis of diabetic complications remains unknown. To investigate the role of leukocyte-derived ROS in periodontitis associated with uncontrolled hyperglycemia, we generated a diabetic mouse strain (Akita/Ncf1) that carried a spontaneous mutation in *INS2* gene resulting in chronic hyperglycemia (Akita mutation) and lacked *p47^{phox}* (Ncf1 null). Here, we report on the chronic lung lesions, increased susceptibility to infection, and decreased survival in Akita/Ncf1 mice.

Materials and Methods

Experimental Animals

Akita mice (C57BL/6-*Ins2^{Akita}*/J, Jackson Laboratories, Bar Harbor, ME) were mated with Ncf1 mice (*p47^{phox}* knockout, Taconic Farm, Germantown, NY) to generate Akita/Ncf1 double mutants. Mice were housed in a temperature- and humidity-controlled room with a 12-hour light-dark cycle where they were kept in sterilized cages with autoclaved water, food, and bedding. All experiments were approved by the Boston University Institutional Animal Care and Use Committee.

Genotyping

PCR was performed using PlatinumTaqDNA Polymerase (Invitrogen, Carlsbad, CA) in GeneAmp PCR System 9700 (Applied Biosystems, Foster City, CA) with the following

primers: Akita forward, 5′-TGCTGATGCCCTGGCCT-GCT-3′; Akita reverse, 5′-TGGTCCCACATATGCACA-TG-3′. Akita PCR products were digested with Fnu4 HI restriction enzyme for 3 hours before gel electrophoresis. Ncf1 primers were as follows: forward, 5′-ACATCAC-AGGCCCCATCATCCTCC-3′; reverse, 5′-GGAGAGC-CCCCTTTCTCTCCCTCA-3′. An additional reverse primer was included in each reaction to detect the following neomycin gene: 5′-CAACGTCGAGCACAGCTGCGCAAG-3′.

Western Blot Analysis

Leukocyte protein extracts were separated by SDS-PAGE (8 μg per lane) on 10% (v/v) polyacrylamide gels. The separated proteins immediately were transferred electrophoretically to a polyvinylidene fluoride membrane. Polyvinylidene fluoride membranes were incubated at 4°C overnight with primary antibodies for $p47^{phox}$ (rabbit anti-mouse purified polyclonal Ab, 1:500 dilution). Antibody binding was detected using horseradish peroxidase—conjugated secondary antibody and enhanced chemiluminescence detection system (Pierce ECL Western Blotting Substrate; Thermo Fisher Scientific, Waltham, MA).

Ligature-Induced Periodontal Disease

Mice were anesthetized using 100 mg/kg ketamine and 5 mg/kg xylazine, injected interperitoneally. A 9-0 silk ligature was tied around the second left maxillary molar, whereas the opposite side was left untreated as control. This allowed for endogenous subgingival biofilm maturation and induction of inflammation-mediated alveolar bone loss.[25] One week later, mice were sacrificed, and the heads were defleshed using a colony of dermestid beetles. Skulls were cleaned with hydrogen peroxide and stained with methylene blue (1%). Alveolar bone loss was measured on digitized microscopic images using image analysis software (Olympus MicroSuite version 3.2.765; Olympus America Inc, Melville, NY).

Lung Histopathology

Each of the mice was euthanized, and a 22-gauge blunt needle was inserted into the exposed trachea. The thorax was opened, and the lungs were inflation-fixed through the injection of 10% formalin in the trachea at a transpulmonary pressure of 25 cm H_2O to ensure proper alveolar dilation. Formalin-fixed lung tissue was embedded in paraffin and sectioned at a thickness of 5 μm on cryostat Micron HM313 (MICROM International GmbH, Waldorf, Germany). Sections of lung were stained with hematoxylin and eosin, periodic acid Schiff (PAS), or Masson's trichrome stain.

Myeloperoxidase Assay

Fresh lungs were weighted and homogenized in an ice-cold protease inhibitor mixture (cOmplete; Sigma-Aldrich, St. Louis, MO) containing 0.005% Triton X in calcium- and magnesium-free phosphate-buffered saline (PBS) using a Dounce Tissue Grinder (Wheaton, Millville, NJ). The tissue was sonicated in 0.1 mmol/L hexadecyltrimethylammonium bromide (Sigma-Aldrich) for 30 seconds and centrifuged at 15,000 × *g* for 15 minutes. Supernatant (20 L) was mixed with 200 μL of assay buffer containing o-Dianisidine HCl, 87.8 mmol/L monobasic potassium phosphate, 12.3 mmol/L dibasic potassium phosphate, and 0.005% hydrogen peroxide and incubated for 2 minutes at room temperature. One hundred fifty microliters of 4N cold sulfuric acid (Fisher Scientific, Fair Lawn, NJ) was added to stop the reaction. Absorbance was read in a microplate reader (SpectraMax 340PC; Molecular Devices, Sunnyvale, CA) at 450 nm optical density at 37°C.

Flow Cytometry of Lung Extracts

Fresh lungs from 8- to 12-week-old male mice were chopped with a sterile scalpel blade and digested with collagenase dispase (1 mg/mL, Sigma-Aldrich) at 37°C for 3 × 20 minutes. Suspended cells were collected by centrifugation and incubated with 50 μg/mL fluorescein isothiocyanate—conjugated LY6G anti-mouse antibody clone 1A8 (eBioscience, San Diego, CA) for 20 minutes. For control experiments, cells were incubated with isotype-matched control antibody. Data were acquired and analyzed on FACScan using Cell Quest Pro software version 5.2 (BD Bioscience, Franklin Lakes, NJ). Debris was excluded on forward and side scatter double parameter dot plots, and doubles were excluded using side scatter pulse height and side scatter pulse width. At least 50,000 gated events were acquired per sample.

Bacterial Cultures

Lung tissue was homogenized in sterilized water using Dounce Tissue Grinder (Wheaton). Serial dilutions (1 to $1/10^5$) from the lung homogenate were prepared, and 20 μL aliquots from each were spread on either Luria-Bertani agar plates or anaerobic blood agar plates (Becton, Dickinson and Company, Franklin Lakes, NY). Luria-Bertani plates were incubated in aerobic condition, whereas blood agar plates were incubated in anaerobic chamber (Coy Laboratory Products, Grass Lake, MI) with 85% nitrogen, 5% hydrogen, and 10% carbon dioxide. Plates were incubated at 37°C for 7 days.

16S Ribosomal RNA Amplification

DNA from lung tissues was extracted with phenol extraction and ethanol precipitation. PCR was performed in a final volume of 50 μL reactions containing 5 μL of 10× reaction buffer, 3 mmol/L $MgCl_2$, 1 μL of dNTPs, 0.2 mmol/L of forward primer and reverse primer, and 1 unit Platinum TaqDNA Polymerase) in GeneAmp PCR System 9700. The reaction mixture contained approximately 50 ng of bacteria template DNA. The 16S rRNA gene was amplified as follows:

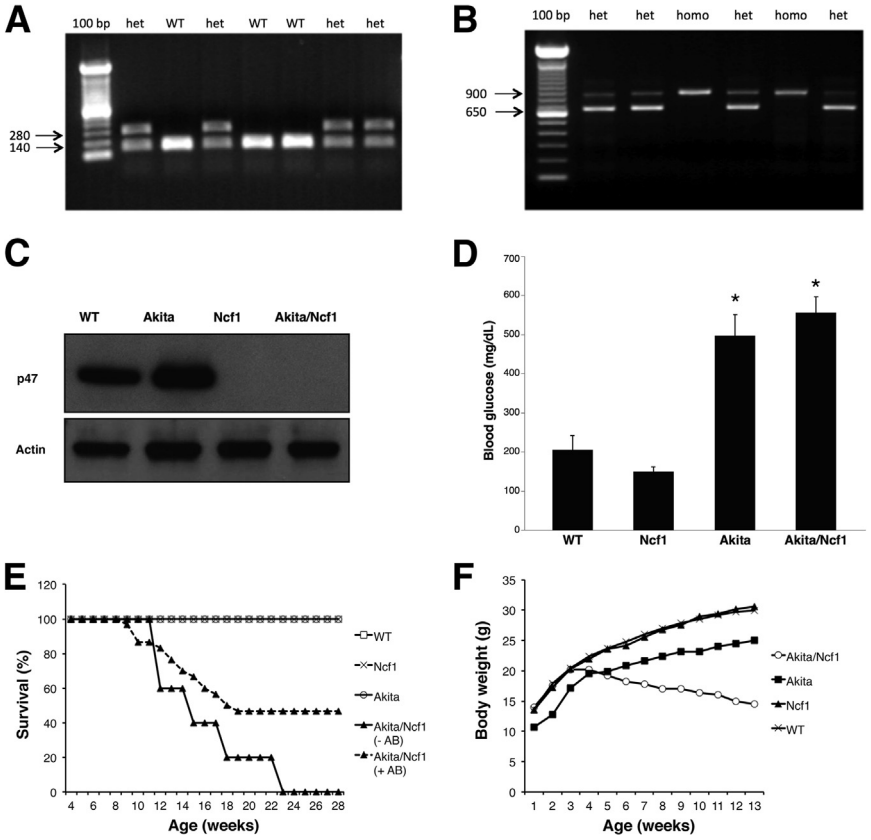

Figure 1 Identification Akita/Ncf1 double mutant mice. **A:** PCR detection of Akita genotype where a point mutation in the *INS2* gene destroys and Fnu4HI restriction site was detected as a 280 bp band with PCR and Fnu4HI restriction enzyme digestion. **B:** PCR detection of Ncf1 genotype. In $Ncf1^{-/-}$ (p47 knockout), the neomycin cassette is detected as a 900 bp band. **C:** Western blot analysis demonstrating the absence of p47 protein in Akita/Ncf1 double mutants. **D:** Blood glucose levels are elevated markedly in Akita and in Akita/Ncf1 mice. **E:** Kaplan/Meyer survival curve showing no death in WT, Akita, and Ncf1 mice in the first 6 months of life. Akita/Ncf1, on the other hand, have 100% mortality rate by 23 weeks in the absence of antibiotic prophylaxis. After administering sulfamethoxazole/trimethoprim antibiotic in the drinking water (+AB) at a concentration of 100 mg/kg per 24 hours, survival increases to 46.3%. Differences between groups were determined by computation of the log rank statistic ($n = 105$). **F:** Progressive weight loss in Akita/Ncf1 mice is demonstrated by monitoring body weight though week 12. Data is presented as means ± SD (**D**). $n = 6$ mice per group (**D**). $^*P < 0.05$, one-way analysis of variance; $P < 0.001$, log rank test (**E**). het, heterozygote for Akita mutation; WT, wild-type.

After a 10-minute denaturation at 94°C, the reaction mixture was run through 35 cycles of denaturation for 1 minute at 94°C, annealing for 1 minute at 55°C, and extension for 2 minutes at 72°C, followed by an incubation for 10 minutes at 72°C. Primers used were forward primer 5′-CCAGCAGCCGCGGTAATACG-3′ corresponding to nucleotides 518 to 537 of *Escherichia coli* 16SrRNA, and reverse primer 5′-ATCGG(C/T)TACCTTGTTACGACTTC-3′ corresponding to nucleotides 1513 to 1491 of the same gene.

Neutrophil Phagocytosis Assay

Interperitoneal injection of 1 mL fluorescein isothiocyanate–labeled zymosan solution (0.5 mg/mL; Invitrogen) in PBS was given to a total of 35 mice [8 wild-type (WT), 10 Ncf1, 5 Akita, and 12 Akita/Ncf1]. Two hours later, after mice were sacrificed by carbon dioxide inhalation followed by cervical dislocation, abdominal lavage was performed to collect neutrophils by retracting the abdominal skin and leaving the abdominal muscles intact. Five milliliters of sterile PBS was injected into the peritoneal cavity using a 22-gauge needle and the lavage fluid withdrawn after gently rubbing the abdomen to wash the recruited immune cells. This was repeated once, injecting a total of 10 mL PBS. The lavage fluid was centrifuged at 1000 × *g* for 10 minutes at room temperature. Cells were then resuspended in 1 mL red blood cell lysis buffer (Invitrogen) for 5 minutes. Cells then were centrifuged at the same conditions mentioned previously and resuspended in 1 mL PBS. Cells were counted in a hemocytometer at 10× magnification using an Olympus CK40-SLP microscope (Olympus, Tokyo, Japan) and fixed in 10% formalin. Neutrophils extracted by injection of nonlabeled zymosan were used as controls. Data were acquired and analyzed on FACScan using CellQuest software. Student's *t*-test was used for statistical analysis.

Bronchoalveolar Lavage

Mice were euthanized by carbon dioxide inhalation, followed by cervical dislocation. Retracting the skin in the neck area exposed the trachea, which was then cannulated, and lungs were lavaged twice with 1 mL of warm Hanks Balanced Salt Solutions (Invitrogen). Both aliquots were centrifuged. The supernatant was discarded, and the cell pellets from both aliquots were resuspended and combined. Total cell counts were obtained using hemocytometer at 10× magnification using an Olympus CK40-SLP microscope. Fifty microliter of the lavage fluid was loaded on cytospin slide and stained with Wright-Giemsa (Sigma-Aldrich) for 1 minute and 200 cell/sample differential counts were performed to determine the absolute numbers of neutrophils. The rest of the lavage fluid was sonicated in 0.1 mol/L hexadecyltrimethylammonium bromide (Sigma-Aldrich) for 30 seconds. The mixture was centrifuged at 15,000 × *g* for 15 minutes. The supernatant from the sonicated fraction was used immediately for myeloperoxidase (MPO) assay as described previously.

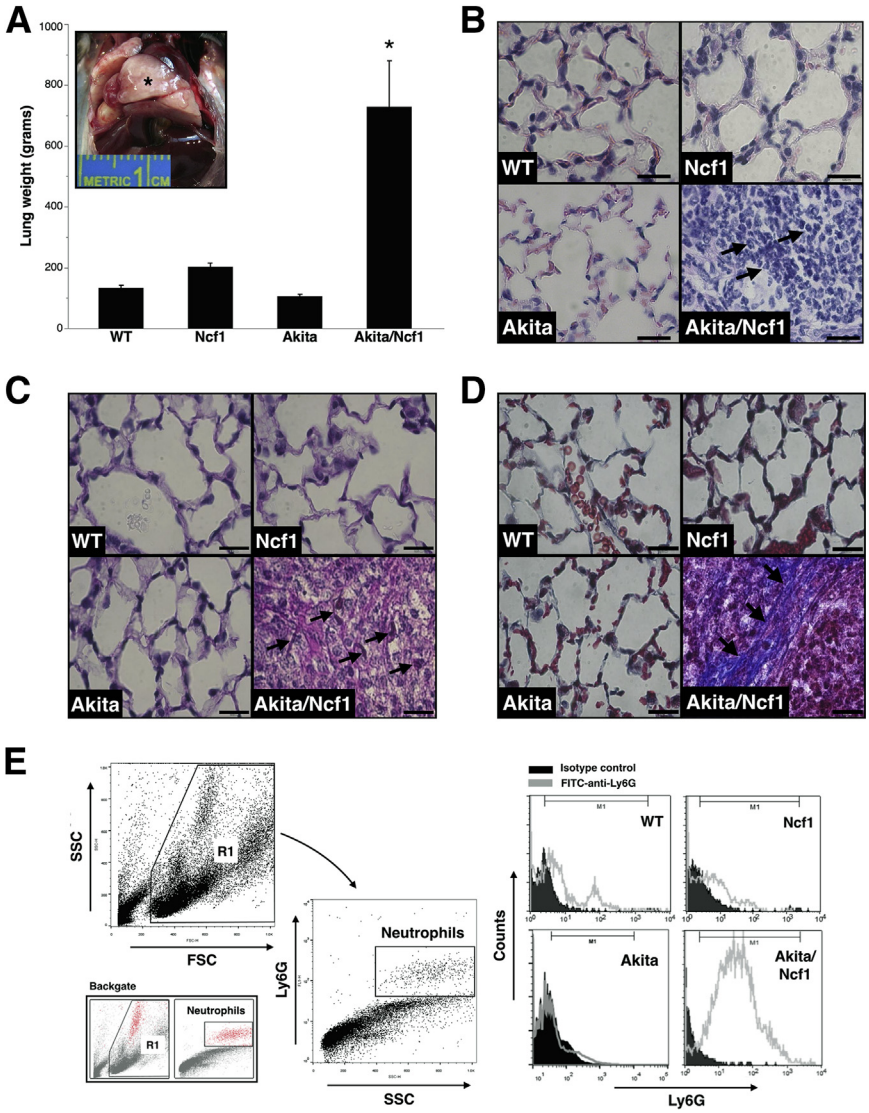

Figure 2 Akita/Ncf1 mice have high mortality rate by 6 months. **A:** Wet lung weight was markedly higher in Akita/Ncf1 male mice. **Inset:** Necropsy of Akita/Ncf1 mice reveals enlarged lungs (**asterisk**) that do not collapse upon opening the thorax. **B:** Representative microscopic images of hematoxylin and eosin—stained lung sections from a terminally ill 12-week-old Akita/Ncf1 male mouse and age- and sex-matched wild-type (WT), Ncf1, and Akita mice are shown. Although WT, Akita, and Ncf1 have normal lung architecture, the Akita/Ncf1 has complete destruction of the lung tissue and obliteration of air spaces with inflammatory cellular infiltrates mostly neutrophils (**arrows**). **C:** Representative histological sections of lungs from a terminally ill Akita/Ncf1 male and matched WT, Ncf1, Akita stained with periodic acid-Schiff. Fungus is detected in Akita/Ncf1 (**arrows**) but not WT, Ncf1, or Akita. **D:** Masson's trichrome staining of lung sections reveals heavy cellular infiltrate, destruction of normal lung tissue, and presence of thick collagen bundles (**arrows**) in the lung of Akita/Ncf1 but not in WT, Akita, or Ncf1 lungs. **E:** Lung neutrophil infiltration is confirmed by flow cytometric analysis of cells released by collagenase/dispase digestion of the lung. Representative histograms of Ly6G expression in lungs of WT, Ncf1, Akita, and Akita/Ncf1 demonstrate a prominent Ly6G-positive (neutrophil) cell population in lungs of Akita/Ncf1. $*P < 0.05$. Scale bars = 20 μm (**B**—**D**).

Neutrophil Degranulation Assay

Lung neutrophils from Akita/Ncf1 males aged 8 to 16 weeks were collected by bronchoalveolar lavage as described previously. The MPO activity from Akita/Ncf1 was compared with a standard curve representing the enzyme activity in WT unstimulated neutrophils. To generate the standard curve, WT mice were injected interperitoneally with 0.1 mg/mL zymosan A, and 2 hours later, cells were collected by peritoneal lavage. Cells were sonicated in 0.1 mol/L hexadecyltrimethylammonium bromide and the supernatant were used to measure the MPO activity. MPO activity was measured from 150×10^4, 15×10^4, and 1.5×10^4 cells, and a standard curve was generated.

Statistical Analysis

Statistical analysis was performed using JMP Pro software version 12 (SAS, Cary, NC). Student's unpaired *t*-tests and one-way analysis of variance were used to compare measurements between genotypes. Flow cytometry data were analyzed using WINMDI software version 2.8 (Dr. Joseph Trotter, Scripps Institute, La Jolla, CA), and mean fluorescence intensity values were compared using Student's unpaired *t*-test. Values of $P < 0.05$ were considered statistically significant.

Results

Akita/Ncf1 Double Mutant Generation

To generate Akita/Ncf1 double mutant mice homozygous *Ncf1*$^{-/-}$, mice were mated with heterozygous Akita$^{+/-}$ mice, because homozygous Akita$^{-/-}$ are infertile. Fifty-seven percent of the first generation offspring (F1) were heterozygous for both the Akita and *Ncf1* genes (Akita$^{+/-}$Ncf1$^{+/-}$). On the other hand, the F2 generation, which were offspring of Akita$^{+/-}$Ncf1$^{+/-}$ F1 mating with Ncf1$^{-/-}$, yielded low litter sizes (3.3 pups per litter), and only 4% of these were the desired double mutant (Akita$^{+/-}$Ncf1$^{-/-}$), a proportion markedly lower than expected (25%) by Mendelian rules

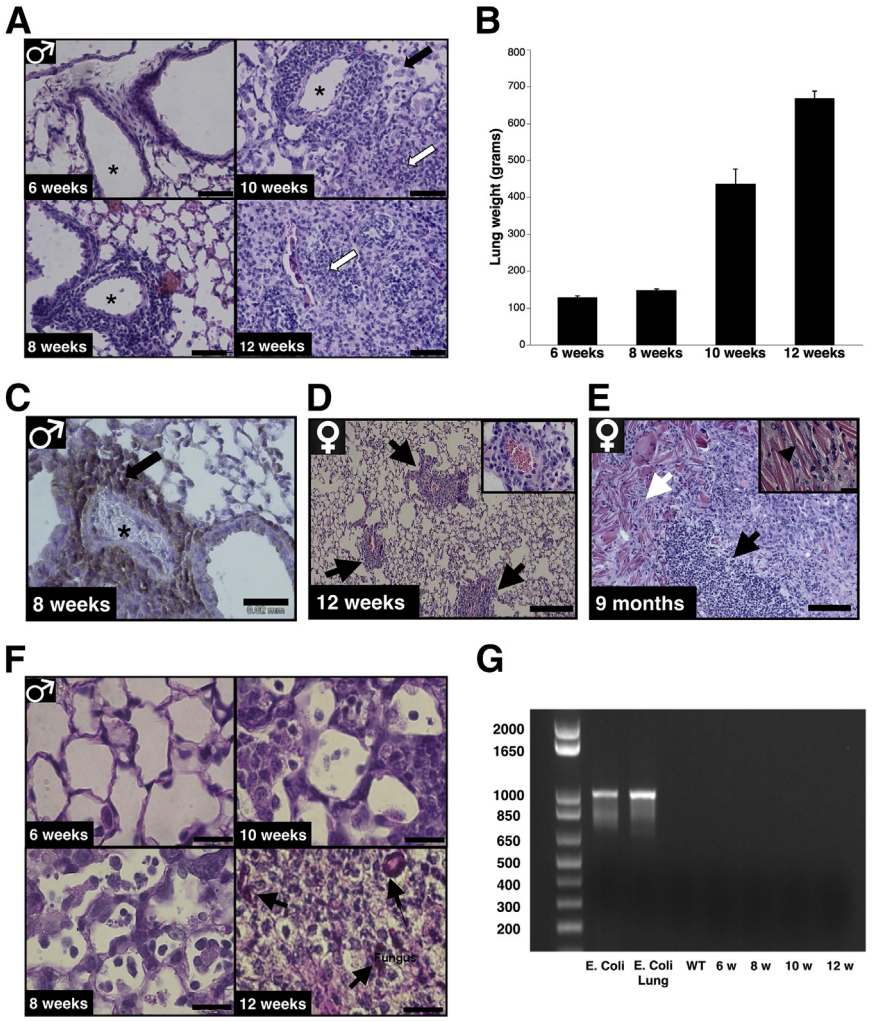

Figure 3 Lack of leukocyte p47 is associated with progressive obstructive lung lesions. **A:** Representative micrographs of hematoxylin and eosin–stained lungs of Akita/Ncf1 male mice at ages 6, 8, 10, and 12 weeks show the progression of cellular lung infiltration over time. Alveolar spaces (**asterisks**) become progressively closed starting at age 8 weeks when cellular infiltrates are observed around arterioles. At 10 weeks, lungs present with a mixed infiltrate containing numerous alveolar macrophages (**black arrow**) and neutrophils (**white arrow**). Lung section from a 12-week-old Akita/Ncf1 mouse shows alveolar space obliterated by neutrophils (**white arrow**). **B:** Lung weights of male Akita/Ncf1 mice increase progressively from age 10 weeks. **C:** Immunohistochemical staining of CD162-positive cells (**arrow**) in the perivascular infiltrate (**asterisk**, blood vessel). **D:** Representative hematoxylin and eosin–stained section of female Akita/Ncf1 lungs at age 12 weeks showing perivascular (**arrows**) mononuclear cell infiltration. Perivascular infiltration at ×40 magnification. **E:** Representative histological lung sections from a 9-month-old Akita/Ncf1 female stained with hematoxylin and eosin illustrating accumulation of extracellular eosinophilic crystalline material (**white arrow**) in the lung parenchyma and inflammatory cell infiltration (**black arrow**). **Inset** shows eosinophilic crystalline material (**black arrowhead**, ×40 magnification). **F:** Periodic acid-Schiff staining of male Akita/Ncf1 lungs revealed fungal infection at 12 weeks (**arrows**) but not at ages 6, 8, and 10 weeks. **G:** PCR for 16S ribosomal RNA in lungs of male Akita/Ncf1 mice revealed no bacterial colonization at ages 6 to 12 weeks. $n = 2$ mice per group (**B**). Scale bar: 0.25 mm (**D**); 20 μm (**A**, **C**, **E**, and **F**).

of inheritance. Further breeding proceeded between Akita$^{+/-}$Ncf1$^{-/-}$ and Ncf1$^{-/-}$. The genotype of the offspring was confirmed by amplification of both *INS2* (Figure 1A) and *Ncf1* genes (Figure 1B) using PCR. Neutrophils from Akita/Ncf1 did not express the p47^{phox} protein as shown with Western blot analysis (Figure 1C). Blood glucose levels were measured at sacrifice to confirm the hyperglycemic phenotype of Akita/Ncf1 double mutants (blood glucose means ± SD: WT, 205 ± 90.5 mg/dL; Ncf1, 149 ± 29.7 mg/dL; Akita, 496.8 ± 132.6 mg/dL; Akita/Ncf1, 555.8 ± 98.3 mg/dL) (Figure 1D).

Akita/Ncf1 Double Mutant Mice Have High Mortality Rate by 20 Weeks of Age

Akita/Ncf1 mice surviving to weaning age (three to four weeks) gradually became cachexic and died by age 23 weeks. Terminally ill male mice had significant weight loss, marked decrease in physical activity, ruffled fur, hunched posture, and labored breathing. Placing mice on antibiotic regimen consisting of sulfamethoxazole/trimethoprim added to the drinking water at a concentration of 100 mg/kg per 24 hours significantly improved the survival of Akita/Ncf1 past 20 weeks. Despite this improvement, a similar low survival rate was observed during the first 20 weeks of age (53.7% mortality rate), with significant sex bias toward males (93.5% of deaths) (Figure 1E). Cachexia was demonstrated by significant and progressive body weight loss from week 4 (Figure 1F). To get more insight into the cause of early death, autopsies were performed on Akita/Ncf1 male mice. Upon dissection, severe enlargement of the lung was noted (Figure 2A). Freshly excised whole wet lung weight was markedly higher in terminally ill Akita/Ncf1 male mice compared with age- and sex-matched WT, Ncf1 null, and Akita mice (lung weight means ± SD: WT, 133.6 ± 23 g; Ncf1, 203 ± 20 g; Akita, 105.8 ± 17.9 g; Akita/Ncf1, 729 ± 262.4 g) (Figure 2A). Histological analysis of lungs of Akita/Ncf1 male mice revealed heavy cellular infiltrate in lung parenchyma with minimal airspace and lack of recognizable alveolar structure. No evidence of structural changes was found in Ncf1 or Akita mice (Figure 2B). Lungs of some terminally ill Akita/Ncf1 male mice were positive for fungus in PAS staining (Figure 2C).

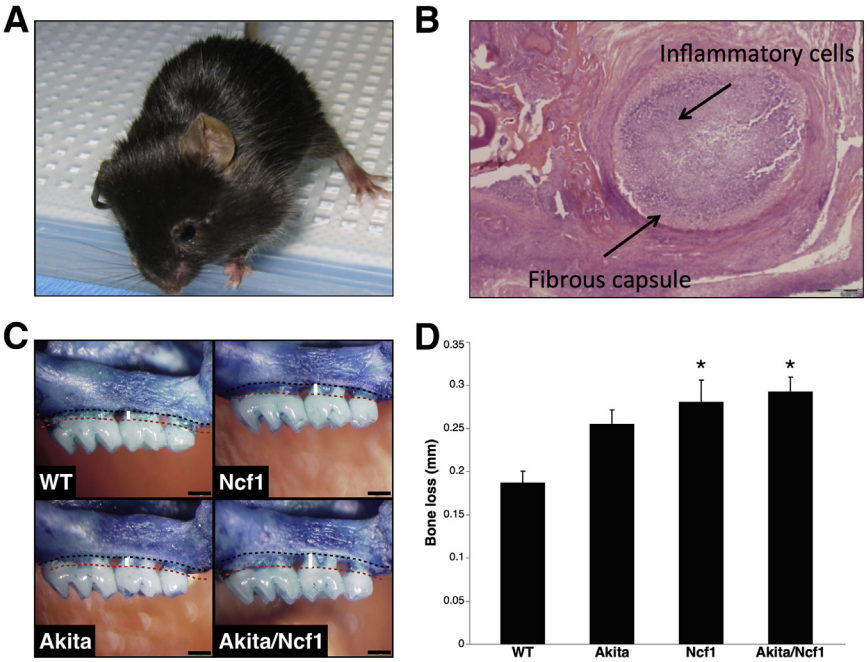

Figure 4 Akita/Ncf1 mice have high susceptibility to oral infections. **A:** Spontaneous abscess formation in Akita/Ncf1 mice in the left submandibular area in the absence of antibiotic prophylaxis. **B:** Hematoxylin and eosin section of a mandibular abscess demonstrating a fibrous capsule surrounding heavy inflammatory cell infiltration. **C:** Ligature-biofilm induced alveolar bone loss as measured as the distance from the cement-enamel junction (**red dotted line**) to the alveolar bone crest (**black dotted line**). Inflammation-mediated bone loss occurs as a result of subgingival biofilms matured from endogenous flora. **D:** Cement-enamel junction–alveolar bone crest distance 3 weeks after placing biofilm-retentive silk ligatures is greater in Akita/Ncf1 mice compared with the other genotypes. Ncf1 and Akita/Ncf1 had significantly higher bone loss compared with wild type (WT). $*P < 0.05$, one-way analysis of variance. $n = 8$ WT, 9 Ncf1, 8 Akita, 8 Akita/Ncf1.

Masson's trichrome staining revealed abundant collagen bundles in the Akita/Ncf1 lung (Figure 2D). Flow cytometric analysis of lung cells released by mincing and collagenase/dispase digestion confirmed that Akita/Ncf1 lungs contained a heavy infiltrate of Ly6G-positive cells (neutrophils) (Figure 2E). Altogether these findings indicated that early death in Akita/Ncf1 mice was only partially caused by infections. The findings also suggested that chronic hyperglycemia with earlier onset in males with Akita mutation may significantly contribute to the high mortality rate in Akita/Ncf1 male mice.

Lung Pathology Develops Prior to Fungal Colonization of Lungs in Akita/Ncf1

To get further insight into the early lung lesions and progression of airway obstruction in Akita/Ncf1 male mice, lung specimens were collected between ages 6 to 12 weeks. Histological analysis was performed on hematoxylin and eosin–stained sections. Lungs of 6-week-old Akita/Ncf1 male mice were smaller compared with WT, but otherwise appeared healthy and had open alveolar spaces with no evident signs of pathology. At 8 weeks of age, inflammatory cell infiltrates were apparent around lung arterioles and bronchioles. Ten-week-old Akita/Ncf1 lungs had mixed cellular infiltrates containing numerous alveolar macrophages and neutrophils extending from the perivascular compartment into the surrounding parenchyma. By 12 weeks, Akita/Ncf1 lungs displayed alveolar spaces obliterated by leukocytes, primarily neutrophils, and fibrosis (Figure 3A). Lung weights increased from 6 to 12 weeks of age concordant to progressive lung infiltration and fibrosis (Figure 3B). Immunohistochemistry for a leukocyte marker of recruitment CD162 (P-selectin glycoprotein ligand 1) was performed. CD162 is expressed primarily by inflammatory monocytes, neutrophils, and Th1 lymphocytes. Many cells of the perivascular infiltrate were positive for CD162 at week 8 (Figure 3C). Akita/Ncf1 females had better survival and slower lung involvement rates compared with males. Histological examination from a 9-month-old female Akita/Ncf1 lung showed severe inflammatory cell infiltration, fibrosis, and air spaces filled with giant eosinophilic extracellular crystals, similar to what was previously reported in Ncf1 mice (Figure 3D). PAS staining was used to detect possible fungal infection causing the observed progressive lung lesions. In lungs of Akita/Ncf1 male mice, PAS-positive structures were found at 12 weeks of age. No fungus was detected in the lung of Akita/Ncf1 males at 6 weeks, 8 weeks, or 10 weeks, indicating that fungal infection occurred on a pre-existing lung lesion that developed earlier (Figure 3E). In addition, 16S PCR on lungs of 6- to 12-week-old Akita/Ncf1 males revealed no bacterial colonization (Figure 3F). Altogether, these findings further suggested that pathogenesis of lung lesions in Akita/Ncf1 is not primarily microbial.

Akita/Ncf1 Have High Incidence of Oral Infections and Severe Biofilm-Induced Bone Loss

Without antibiotic prophylaxis, 60% ($n = 71$) of Akita/Ncf1 mice developed spontaneous abscesses in the head and neck region (Figure 4A). The prevalence of oral abscesses was decreased significantly to 23.4% ($n = 25$) with antibiotic treatment. Lesions were most commonly unilateral

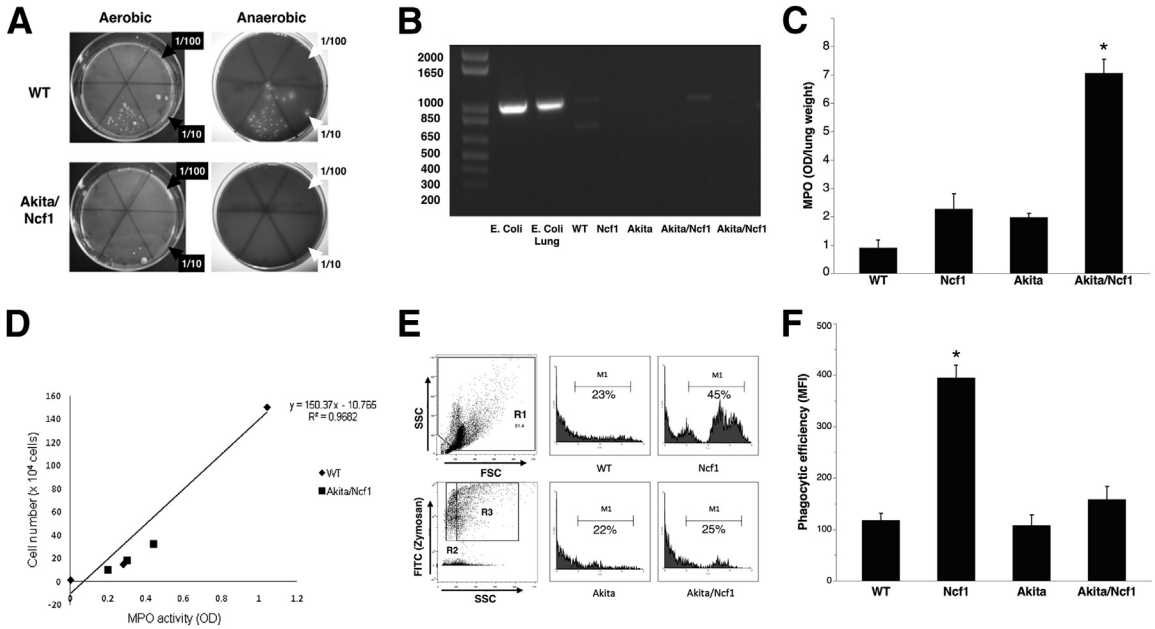

Figure 5 Neutrophil infiltration in Akita/Ncf1 lungs does not correlate with bacterial colonization. **A:** Culturing lung homogenates under aerobic or anaerobic conditions yielded no more bacteria in terminally ill male Akita/Ncf1 mice compared with age- and sex-matched wild type (WT). The sextants in the culture plates indicate serial dilutions of lung homogenate (0, 1/10 to $1/10^5$). The lower middle sextant in each plate received undiluted sample. **B:** 16S ribosomal RNA amplification by PCR. Positive controls include DNA extracts from *Escherichia coli* (*E. coli*) and WT lung injected with *E. coli* (*E. coli* lung). Lung samples from two terminally ill Akita/Ncf1 male mice and one of each genotype WT, Ncf1, and Akita are shown (experiment run in duplicate). **C:** Lung neutrophil infiltration in terminally ill Akita/Ncf1 mice was measured using a myeloperoxidase (MPO) assay. Akita/Ncf1 has significantly higher lung MPO levels compared with all other genotypes. **D:** Neutrophil degranulation in Akita/Ncf1 was assessed on lung neutrophils collected by bronchoalveolar lavage. Cells were sonicated to release MPO present in the intracellular primary granules. Levels of MPO in the supernatant was measured and compared with the standard curve generated from unstimulated WT neutrophil MPO levels. **E:** Phagocytic efficiency was assessed *in vivo* by inducing acute peritonitis with fluorescein isothiocyanate–labeled zymosan A. Debris was excluded on forward scatter versus side scatter dot plots (R1). Representative flow cytometry histogram analysis of zymosan uptake by phagocytes from WT, Ncf1, Akita, and Akita/Ncf1 is shown. Shaded area within M1 (marker) represents phagocytosed fluorescein isothiocyanate–labeled zymosan particles (equivalent to R3). Unlabelled zymosan was used as control and presented as the shaded area on the right outside the marker area (equivalent to R2). **F:** Comparison of phagocytic efficiency showed no difference for Akita and Akita/Ncf1 compared with WT. However, a marked increase in phagocytic efficiency was observed in Ncf1. Data represent geometric means for M1 $*P < 0.05$, one-way analysis of variance. $n = 4$ Akita/Ncf1 (**B**), 12 (**F**); $n = 5$ Akita (**F**); $n = 5$ per group (**C**); $n = 8$ WT (**F**); $n = 10$ Ncf1 (**F**).

and related to either the maxilla or the mandible. None of the WT, Ncf1, or Akita mice presented with abscesses in the orofacial region. Histological analysis of orofacial tissues revealed a heavy neutrophil infiltrate surrounded by a fibrous capsule, indicative of a nonresolving acute inflammation (Figure 4B). To get further insight into the innate immune response to oral biofilms in diabetic mice deficient in leukocyte superoxide, we used a model of periodontitis, a known complication of diabetes in humans. Placement of a biofilm-retentive silk suture in the gingival sulcus of molars results in maturation of subgingival biofilms from endogenous flora that induces local inflammation and alveolar bone loss around teeth. Ligatures were placed in 6- to 9-week-old age- and sex-matched WT, Ncf1, Akita, and Akita/Ncf1 mice. Ligatures were left in place for 21 days, and bone levels were measured and compared with the contralateral healthy side. Induction of acute periodontal disease in Akita/Ncf1 mice by ligation of a 9-0 silk suture around the upper left second molar resulted in significantly higher alveolar bone loss compared with WT mice as measured with the cement-enamel junction–alveolar bone crest distance (WT, 0.2 ± 0.03 mm; Ncf1, 0.28 ± 0.07 mm, Akita, 0.27 ± 0.05 mm; Akita/Ncf1, 0.29 ± 0.05 mm; means $\pm$ SD) (Figure 4, C and D). Loss of bone was similar in Akita/Ncf1, Akita and Ncf1 mice ($n = 8$ WT, 9 Ncf1, 8 Akita, 8 Akita/Ncf1).

High Lung Neutrophil Infiltration Is Associated with Minimal Bacterial Colonization in Akita/Ncf1 Mice

To elucidate whether the neutrophil infiltrates are indicative of bacterial lung infection in Akita/Ncf1 mice, lung homogenates from 12-week-old terminally ill Akita/Ncf1 double mutant mice and aged-matched WT mice were cultured on agar plates for 7 days. Serial dilutions of lung homogenate supernatants were plated on Luria-Bertani–agar or blood agar plates and incubated under aerobic or anaerobic conditions, respectively. WT cultures resulted in bacterial growth from the undiluted and from the 1/10 diluted lung homogenate under both aerobic and anaerobic conditions (Figure 5A). Akita/Ncf1 lung homogenates yielded bacterial growth only in the undiluted samples. This indicated no more bacteria in Akita/Ncf1 double mutants than in WT. A more comprehensive approach to

bacteria detection was used with bacterial 16S ribosomal RNA amplification. DNA extracts from the lungs of terminally ill Akita/Ncf1 as well as from the lungs of age-matched WT, Ncf1, and Akita were amplified using 16S ribosomal RNA-specific primers. WT lungs injected with *E. coli* were used as positive control. WT lung DNA extracts displayed the expected approximately 1 kb band, matching those from the positive controls (Figure 5B). Akita/Ncf1 lung DNA amplification yielded weaker 16S signal, confirming the bacterial culture results (experiment run in duplicate, $n = 4$ Akita/Ncf1 mice).

Despite similar bacterial colonization in the lung in WT and Akita/Ncf1, levels of MPO, an enzyme abundant in neutrophils, were markedly higher in Akita/Ncf1 lung homogenates (MPO optical density/lung weight means ± SD: WT, 0.9 ± 0.54; Ncf1, 2.27 ± 1.07; Akita, 1.98 ± 0.25; Akita/Ncf1, 7.06 ± 0.97; $n = 4$ mice/group) (Figure 5C). To determine whether neutrophils in Akita/Ncf1 lung are undergoing excessive degranulation, thus contributing to the lung destruction, neutrophils from Akita/Ncf1 males were collected, lyzed, and the level of MPO remaining in the granules was quantified. This was compared with standard curve defined by the amount of MPO enzyme present in the granules of unstimulated neutrophils from WT. Neutrophils recruited into the lungs of Akita/Ncf1 showed similar degranulation compared with unstimulated WT neutrophils (MPO means ± SD: WT, 0.28 per 1.5×10^4 cells; Akita/Ncf1, 0.2 per 1.0×10^4 cells, 0.3 per 1.8×10^4 cells, and 0.45 per 3.2×10^4 cells) (Figure 5D). Phagocytic efficiency was assessed by flow cytometry after inducing acute peritonitis with fluorescent-labeled zymosan A particles. Ncf1 mice had significantly higher phagocytic efficiency compared with the other genotypes. There was no difference in phagocytic efficiency between Akita/Ncf1 and WT mice (means ± SD mean fluorescence intensity: WT, 117.6 ± 37.5; Ncf1, 394.7 ± 76; Akita, 107.9 ± 44.6; Akita/Ncf1, 158.3 ± 88.1) (Figure 5, E and F).

Discussion

The present study demonstrates that inactivating the source of leukocyte ROS in mice with chronic hyperglycemia results in high prevalence of oral abscesses, progressive interstitial inflammation, and fibrosis in the lung, leading to cachexia and death. These findings indicate that the NADPH-oxidase generated ROS is not only beneficial but also essential to oral and respiratory health in diabetes, particularly when the disease is uncontrolled. These observations were made in the complete absence of leukocyte ROS in mice with uncontrolled chronic hyperglycemia. The specific time points chosen for our study were made on the basis of our observation that Akita/Ncf1 males start losing weight around eight weeks of age. In the absence of evident bacterial or fungal infection, Akita/Ncf1 male lungs had notable pathological changes characterized by perivascular and peribronchiolar inflammatory cell infiltration and fibrosis as early as six weeks of age.

The relative contribution of chronic hyperglycemia and lack of leukocyte $p47^{phox}$ to the development of inflammatory lung infiltration and fibrosis may be explained by previous findings in Ncf1 mice.[26] The absence of leukocyte $p47^{phox}$ in Ncf1 mice protected them against bleomycin-induced pulmonary fibrosis despite heavy pulmonary neutrophil infiltration compared with WT mice.[26] However, the excessive release of proteolytic enzymes by neutrophils play important roles in the pathogenesis of acute and chronic obstructive or restrictive lung diseases.[27–29] In our study, Akita/Ncf1 mice had spontaneous neutrophil lung infiltration without excessive degranulation of primary granules. Interestingly, the infiltrative lung lesions start developing in Akita/Ncf1 male mice between six to eight weeks of age, soon after Akita male mice show progressive decrease in β cell mass density and increasing blood glucose levels (four to six weeks of age).[20] Concordant to this association, Akita/Ncf1 females start developing lung lesions later (around 12 weeks of age) and have better survival rates, likely because of the delayed onset of and less severe hyperglycemia compared with males, which is known for Akita mice. Additionally, Ncf1 mice do not develop lung lesions at an early age.[30] Nonetheless, the addition of an antibiotic to the drinking water only partially improved survival, suggesting that infection only accounts for terminal complications in some mice and, in the context of similar high blood glucose levels, in all Akita/Ncf1 mice. Consistent with this finding, there was no overt bacterial load in the lungs of terminally ill Akita/Ncf1 compared with age-matched WT, Ncf1, or Akita mice.

Hyperglycemia appears to be a predisposing factor for lung fibrosis in Akita/Ncf1, as single-mutant Akita mice maintained patent lung air spaces and showed no signs of fibrosis. A possible explanation for this finding is that healing of chronic lung inflammation is diverted toward a fibrotic phenotype by chronic hyperglycemia. Pathogenesis of fibrosis in diabetes was associated with overproduction of prosclerotic cytokines, such as TGF-β1 and connective tissue growth factor, and imbalances in protease or antiprotease systems that result in excess extracellular matrix deposition.[31] Interestingly, extracellular crystalline material was detected in the lungs of aging Akita/Ncf1 females, but not in males, possibly because of the shorter life span of male Akita/Ncf1 mice. Similar crystal formation was described in the lungs of Ncf1 mice with or without evidence of infection.[30,32] The crystal in Ncf1 mice was identified as Ym1/Ym2 protein, a chitinase-like lectin that is expressed transiently during developmental hematopoiesis, inflammatory responses to chemical or traumatic stimuli, and by alternatively activated macrophages during T helper-2 biased immune responses. The function of Ym1/Ym2 proteins is not fully understood, but it was suggested to be involved in host immune defense.[33] No similar crystal formation was reported in the lungs of patients with CGD or diabetes. However, patients with CGD have a high incidence of

autoimmune diseases, such as inflammatory bowel syndrome, rheumatoid arthritis, and sarcoidosis.[34] Similar crystalline lesion was described in mice of the C57BL/6 and 129Sv strain as well as in knockout mice on those backgrounds.[35,36]

The progression of interstitial lung lesions from age eight weeks, before detection of fungus and in the absence of significant bacterial colonization, suggests an intrinsic immune-mediated type of interstitial pneumonia developing in diabetic mice lacking $p47^{phox}$. Myeloid-lymphoid lung infiltration and areas of fibrosis observed in Akita/Ncf1 mice suggest a diagnosis of idiopathic interstitial pneumonia, which is associated generally with immune incompetence or autoimmunity.[37] Antibiotic treatment supplied in drinking water prolonged but did not normalize survival, indicating that bacteria contributed to decreased survival in Akita/Ncf1 mice and that infection likely was superposed on pre-existing lung lesions leading to early death in some cases. Previous studies have shown that both diabetes and CGD increase the susceptibility to developing potentially life-threatening bacterial infections.[38,39] Recurrent fungal pulmonary infection with *Aspergillus spp*. is the most common cause of death in patients in CGD.[40] Single mutant Ncf1 mouse are highly susceptible to lung aspergillosis, and intratracheal inoculation of Ncf1 mice with *Aspergillus fumigatus* (10^4 colony-forming units per mouse) induces massive neutrophil infiltrate and death, similar to what was observed in the unchallenged Akita/Ncf1 mice.[41] In our study, fungal growth was detected with PAS staining in the lung of Akita/Ncf1 mice by 12 weeks of age. In addition, oral infections were more prevalent and severe in Akita/Ncf1 mice, as demonstrated by spontaneous abscesses and more severe loss of alveolar bone in response to biofilm-retentive ligatures placed around molars. One explanation for increased susceptibility to infection is the impaired innate immune response to opportunistic infectious agents in endogenous oral flora. Interestingly, Ncf1 null phagocytes (neutrophils and macrophages) exhibited increased phagocytic efficiency, possibly as a compensatory mechanism for their inability to produce ROS. In addition to ROS, the neutrophils use proteolytic antimicrobial molecules (including lactoferrin, lysozyme, β2-microglobulin, collagenase and gelatinase, histaminase, heparinase, and sialidase) released into the acidic milieu of phagosomes.[42] Akita mutation, however, reduced phagocytic efficiency in Akita/Ncf1 mice to levels comparable with WT mice. Therefore the ability of phagocytes to control biofilm pathogenicity may be impaired by chronic hyperglycemia in Akita/Ncf1 mice.

Pathogenic subgingival biofilms likely are controlled by efficient innate immune responses that maintain a balance between aggregates of physiologically compatible organisms and an immune-inflammatory state associated with proinflammatory mediators inside periodontal tissues. Altered innate immune circuits are associated with dysbiosis and pro-osteolytic environments that lead to bone loss around teeth. This is referred to as polymicrobial synergy and dysbiosis model of periodontitis pathogenesis.[43,44] Therefore, using a mouse model of periodontitis, in which subgingival biofilms formed from endogenous flora mature when undisturbed (similar to what is seen in humans), offered us the possibility to investigate critical immune regulatory factors in biofilm control, such as neutrophil ROS production. Although patients with CGD do not have increased susceptibility to periodontitis, the prevalence and severity of periodontitis is increased in patients with diabetes,[45,46] and control of blood glucose as measured with glycated hemoglobin (HbA1c) levels correlates with the severity of periodontal tissue breakdown.[23] Akita mice respond to molar ligation with accelerated periodontal bone loss.[21] Microvascular changes and deposition of advanced glycation end-products in gingival microvasculature associated with uncontrolled hyperglycemia contribute to the more severe phenotype in diabetic mice.[8,9,47] In the current study, double mutant Akita/Ncf1 showed only slightly higher levels of root exposure. Although previous research showed that excess neutrophil-derived ROS contributes to bone loss in periodontitis,[48] the present study indicates that lack of ROS in leukocytes also may be detrimental to periodontal health. This supports the concept that a balance between oxidants and antioxidants is required for maintenance of periodontal health.

Altogether, the present study demonstrates that chronic hyperglycemia combined with leukocyte deficiency in ROS production is associated with cachexia, interstitial pneumonia, and susceptibility to infections. These findings contribute to our understanding of altered innate immune pathways associated with diabetes.

Acknowledgments

We thank Daniel Remick (Boston University, Boston, MA) for helpful discussions.

M.F.Z. performed experiments and contributed to discussion, C.S. performed experiments and wrote the manuscript; K.S. and N.F. performed experiments; M.G. reviewed the manuscript; T.E.V.D. contributed to discussion and reviewed manuscript; R.G. contributed to discussion and wrote the manuscript.

References

1. Centers for Disease Control and Prevention: National diabetes fact sheet: national estimates and general information on diabetes and prediabetes in the United States. 2011. Atlanta, GA: US Department of Health and Human Services, Centers for Disease Control and Prevention; 2011. Available at www.cdc.gov/diabetes/pubs/pdf/ndfs_2011.pdf (accessed June 16, 2015)
2. Mealey BL, Ocampo GL: Diabetes mellitus and periodontal disease. Periodontology 2000 2007, 44:127−153
3. Soskolne WA, Klinger A: The relationship between periodontal diseases and diabetes: an overview. Ann Periodontol 2001, 6: 91−98
4. Taylor G, Borgnakke W: Periodontal disease: associations with diabetes, glycemic control and complications. Oral Dis 2008, 14:191−203
5. Chawla A, Nguyen KD, Goh YPS: Macrophage-mediated inflammation in metabolic disease. Nat Rev Immunol 2011, 11:738−749

6. Vandanmagsar B, Youm Y-H, Ravussin A, Galgani JE, Stadler K, Mynatt RL, Ravussin E, Stephens JM, Dixit VD: The NLRP3 inflammasome instigates obesity-induced inflammation and insulin resistance. Nat Med 2011, 17:179–188
7. Snell-Bergeon JK, West NA, Mayer-Davis EJ, Liese AD, Marcovina SM, D'Agostino RB, Hamman RF, Dabelea D: Inflammatory markers are increased in youth with Type 1 Diabetes: the SEARCH Case-Control Study. J Clin Endocrinol Metab 2010, 95: 2868–2876
8. Lalla E, Lamster IB, Feit M, Huang L, Spessot A, Qu W, Kislinger T, Lu Y, Stern DM, Schmidt AM: Blockade of RAGE suppresses periodontitis-associated bone loss in diabetic mice. J Clin Invest 2000, 105:1117–1124
9. Lalla E, Lamster IB, Drury S, Fu C, Schmidt AM: Hyperglycemia, glycoxidation and receptor for advanced glycation endproducts: potential mechanisms underlying diabetic complications, including diabetes-associated periodontitis. Periodontology 2000 2000, 23: 50–62
10. Yoshioka M, Kayo T, Ikeda T, Koizumi A: A novel locus, Mody4, distal to D7Mit189 on chromosome 7 determines early-onset NIDDM in nonobese C57BL/6 (Akita) mutant mice. Diabetes 1997, 46:887–894
11. Brownlee M: Biochemistry and molecular cell biology of diabetic complications. Nature 2001, 414:813–820
12. Nishikawa T, Edelstein D, Brownlee M: The missing link: a single unifying mechanism for diabetic complications. Kidney Int Suppl 2000, 77:S26–S30
13. Yao D, Brownlee M: Hyperglycemia-induced reactive oxygen species increase expression of the receptor for advanced glycation end products (RAGE) and RAGE ligands. Diabetes 2010, 59: 249–255
14. Valko M, Leibfritz D, Moncol J, Cronin MTD, Mazur M, Telser J: Free radicals and antioxidants in normal physiological functions and human disease. Int J Biochem Cell Biol 2007, 39:44–84
15. Balaban RS, Nemoto S, Finkel T: Mitochondria, oxidants, and aging. Cell 2005, 120:483–495
16. Valavanidis A, Vlachogianni T, Fiotakis C: 8-hydroxy-2′ -deoxyguanosine (8-OHdG): a critical biomarker of oxidative stress and carcinogenesis. J Environ Sci Health C Environ Carcinog Ecotoxicol Rev 2009, 27:120–139
17. Iglesias-de la Cruz MC, Ruiz-Torres P, Alcamí J, Díez-Marqués L, Ortega-Velázquez R, Chen S, Rodríguez-Puyol M, Ziyadeh FN, Rodríguez-Puyol D: Hydrogen peroxide increases extracellular matrix mRNA through TGF-β in human mesangial cells. Kidney Int 2001, 59: 87–95
18. Ha H, Lee HB: Reactive oxygen species as glucose signaling molecules in mesangial cells cultured under high glucose. Kidney Int Suppl 2000, 77:S19–S25
19. Ha H, Lee HB: Reactive oxygen species amplify glucose signalling in renal cells cultured under high glucose and in diabetic kidney. Nephrology 2005, 10:S7–S10
20. Lee HB, Yu M-R, Yang Y, Jiang Z, Ha H: Reactive oxygen species-regulated signaling pathways in diabetic nephropathy. J Am Soc Nephrol 2003, 14:S241–S245
21. Nauseef WM, Borregaard N: Neutrophils at work. Nat Immunol 2014, 15:602–611
22. Gyurko R, Siqueira CC, Caldon N, Gao L, Kantarci A, Van Dyke TE: Chronic hyperglycemia predisposes to exaggerated inflammatory response and leukocyte dysfunction in Akita mice. J Immunol 2006, 177:7250–7256
23. Karima M, Kantarci A, Ohira T, Hasturk H, Jones VL, Nam B-H, Malabanan A, Trackman PC, Badwey JA, Van Dyke TE: Enhanced superoxide release and elevated protein kinase C activity in neutrophils from diabetic patients: association with periodontitis. J Leukoc Biol 2005, 78:862–870
24. Omori K, Ohira T, Uchida Y, Ayilavarapu S, Batista EL, Yagi M, Iwata T, Liu H, Hasturk H, Kantarci A, Van Dyke TE: Priming of neutrophil oxidative burst in diabetes requires preassembly of the NADPH oxidase. J Leukoc Biol 2008, 84:292–301
25. Sima C, Gastfreund S, Sun C, Glogauer M: Rac-null leukocytes are associated with increased inflammation-mediated alveolar bone loss. Am J Pathol 2014, 184:472–482
26. Manoury B, Nenan S, Leclerc O, Guenon I, Boichot E, Planquois J-M, Bertrand CP, Lagente V: The absence of reactive oxygen species production protects mice against bleomycin-induced pulmonary fibrosis. Respir Res 2005, 6:11
27. Lee WL, Downey GP: Leukocyte elastase: physiological functions and role in acute lung injury. Am J Respir Crit Care Med 2001, 164: 896–904
28. Nadel JA: Role of neutrophil elastase in hypersecretion during COPD exacerbations, and proposed therapies. Chest J 2000, 117: 386S–389S
29. Geerts L, Jorens PG, Willems J, De Ley M, Slegers H: Natural inhibitors of neutrophil function in acute respiratory distress syndrome. Crit Care Med 2001, 29:1920–1924
30. Ban CR, Twigg SM: Fibrosis in diabetes complications: pathogenic mechanisms and circulating and urinary markers. Vasc Health Risk Manag 2008, 4:575–596
31. Harbord M, Novelli M, Canas B, Power D, Davis C, Godovac-Zimmermann J, Roes J, Segal AW: Ym1 is a neutrophil granule protein that crystallizes in p47phox-deficient mice. J Biol Chem 2002, 277:5468–5475
32. Jackson SH, Gallin JI, Holland SM: The p47phox mouse knock-out model of chronic granulomatous disease. J Exp Med 1995, 182: 751–758
33. Guo L, Johnson RS, Schuh JC: Biochemical characterization of endogenously formed eosinophilic crystals in the lungs of mice. J Biol Chem 2000, 275:8032–8037
34. De Ravin SS, Naumann N, Robinson MR, Barron KS, Kleiner DE, Ulrick J, Friend J, Anderson VL, Darnell D, Kang EM, Malech HL: Sarcoidosis in chronic granulomatous disease. Pediatrics 2006, 117: e590–e595
35. Milner JD, Ward JM, Keane-Myers A, Paul WE: Lymphopenic mice reconstituted with limited repertoire T cells develop severe, multiorgan, Th2-associated inflammatory disease. Proc Natl Acad Sci U S A 2007, 104:576–581
36. Ward JM, Yoon M, Anver MR, Haines DC, Kudo G, Gonzalez FJ, Kimura S: Hyalinosis and Ym1/Ym2 gene expression in the stomach and respiratory tract of 129S4/SvJae and wild-type and CYP1A2-null B6, 129 mice. Am J Pathol 2001, 158:323–332
37. Cha S-I, Fessler MB, Cool CD, Schwarz MI, Brown KK: Lymphoid interstitial pneumonia: clinical features, associations and prognosis. Eur Respir J 2006, 28:364–369
38. Assari T: Chronic Granulomatous Disease; fundamental stages in our understanding of CGD. Med Immunol 2006, 5:4
39. Wheat LJ: Infection and diabetes mellitus. Diabetes Care 1980, 3: 187–197
40. Winkelstein JA, Marino MC, Johnston RB, Boyle J, Curnutte J, Gallin JI, Malech HL, Holland SM, Ochs H, Quie P, Buckley RH, Foster CB, Chanock SJ, Dickler H: Chronic granulomatous disease. Report on a national registry of 368 patients. Medicine (Baltimore) 2000, 79:155–169
41. Dennis CG, Greco WR, Brun Y, Youn R, Slocum HK, Bernacki RJ, Lewis R, Wiederhold N, Holland SM, Petraitiene R, Walsh TJ, Segal BH: Effect of amphotericin B and micafungin combination on survival, histopathology, and fungal burden in experimental aspergillosis in the p47phox-/- mouse model of chronic granulomatous disease. Antimicrob Agents Chemother 2006, 50:422–427
42. Sima C, Glogauer M: Neutrophil dysfunction and host susceptibility to periodontal inflammation: current state of knowledge. Curr Oral Health Rep 2014, 1:95–103
43. Hajishengallis G, Lamont RJ: Beyond the red complex and into more complexity: the polymicrobial synergy and dysbiosis (PSD)

model of periodontal disease etiology. Mol Oral Microbiol 2012, 27: 409–419
44. Hajishengallis G: Immunomicrobial pathogenesis of periodontitis: keystones, pathobionts, and host response. Trends Immunol 2014, 35:3–11
45. Fontana G, Lapolla A, Sanzari M, Piva E, Mussap M, De Toni S, Plebani M, Fusetti F, Fedele D: An immunological evaluation of type II diabetic patients with periodontal disease. J Diabetes Complications 1999, 13:23–30
46. Grossi SG, Skrepcinski FB, DeCaro T, Robertson DC, Ho AW, Dunford RG, Genco RJ: Treatment of periodontal disease in diabetics reduces glycated hemoglobin. J Periodontol 1997, 68: 713–719
47. Sima C, Rhourida K, Van Dyke TE, Gyurko R: Type 1 diabetes predisposes to enhanced gingival leukocyte margination and macromolecule extravasation in vivo. J Periodontal Res 2010, 45: 748–756
48. Battino M, Bullon P, Wilson M, Newman H: Oxidative injury and inflammatory periodontal diseases: the challenge of anti-oxidants to free radicals and reactive oxygen species. Criti Rev Oral Bio Med 1999, 10:458–476